

Sub-diffraction limited imaging with fluorophores exhibiting emission depletion upon saturation

Assaf Avidan and Dan Oron

Weizmann Institute of Science, Department of Complex System, Rehovot, Israel

assaf.avidan@weizmann.ac.il

Abstract: We present a simplified single-beam scheme for depletion-based sub-diffraction-limited imaging which allows for less restrictive illumination conditions. This is done by introducing the concept of fluorophores exhibiting emission depletion upon saturation. We discuss the circumstances under which such a depletion based process is possible, and derive the scaling of the spatial resolution utilizing this scheme. Next, we analyze the proper illumination conditions both in space and time required for sub diffraction limited imaging, and show that it is applicable only under pulsed excitation. Finally, our scheme's advantages and shortcomings relative to alternative realizations of depletion-based sub-diffraction-limited microscopy are discussed.

© 2008 Optical Society of America

OCIS codes: (180.2520) Fluorescence microscopy.

References and links

1. S. W. Hell, "Far field optical nanoscopy," *Science* **316**, 1153-1158 (2007).
2. R. W. Boyd, "*Nonlinear Optics*," second edition, (Academic Press, 2003).
3. M. J. Rust, M. Bates, and X. Zhuang, "Sub-diffraction-limit imaging by stochastic optical reconstruction microscopy (STORM)," *Nat. Methods* **3**, No. 10, 793-796 (2006).
4. M. Bates, B. Huang, G. T. Dempsey, and X. Zhuang, "Multicolor Super-Resolution Imaging with Photo-Switchable Fluorescent Probes," *Science* **317**, 1749-1753 (2007).
5. E. Betzig, G. H. Patterson, R. Sougrat, O. W. Lindwasser, S. Olenych, J. S. Bonifacino, M. W. Davidson, J. Lippincott-Schwartz, and H. F. Hess, "Imaging Intracellular Fluorescent Proteins at Nanometer Resolution," *Science* **313**, 1642-1645 (2006).
6. S. T. Hess, T. P. K. Girirajan, and M. D. Mason, "Ultra-High Resolution Imaging by Fluorescence Photoactivation Localization Microscopy," *Biophys. J.* **91**, 4258-4272 (2006).
7. A. Sharonov and R. M. Hochstrasser, "Wide-Field Subdiffraction Imaging by Accumulated Binding of Diffusing Probes," *Proc. Natl. Acad. Sci.* **103**, No. 50, 18911-18916 (2006).
8. H. Bock, C. Geisler, C. A. Wurm, C. von Middendorff, S. Jakobs, A. Schonle, A. Egner, S. W. Hell, and C. Eggeling, "Two-Color Far-Field Fluorescence Nanoscopy Based on Photoswitchable Emitters," *Appl. Phys. B* **88**, 161-165 (2007).
9. A. Egner, C. Geisler, C. von Middendorff, H. Bock, D. Wenzel, R. Medda, M. Andresen, A. C. Stiel, S. Jakobs, C. Eggeling, A. Schonle, and S. W. Hell, "Fluorescence Nanoscopy in Whole Cells by Asynchronous Localization of Photoswitching Emitters," *Biophys. J.* **93** No. 11, 3285-3290 (2007).
10. S. W. Hell and J. Wichmann, "Breaking the diffraction limit by stimulated emission: Stimulated emission sincdepletion microscopy," *Opt. Lett.* **19** 780-782, (1994).
11. K. I. Willing, B. Harke, R. Medda, and S. W. Hell, "STED microscopy with continuous wave beams," *Nat. Methods* **4**, No. 11, 915-918 (2007).
12. S. E. Irvine, T. Staudt, E. Rittweger, J. Engelhardt, and S. W. Hell, "Direct Light-Driven Modulation of Luminescence from Mn-Doped ZnSe Quantum Dots," *Angew. Chem. Int. Ed.* **47**, Vol. 14, 2685-2688 (2008).
13. S. Bretschneider, C. Eggeling, and S. W. Hell, "Breaking the Diffraction Barrier in Fluorescence Microscopy by Optical Shelving," *Phys. Rev. Lett.* **98**, 218103(1-4) (2007).

14. G. Donnert, J. Keller, C. A. Wurm, S. O. Rizzoli, V. Westphal, A. Schonle, R. Jahn, S. Jakobs, C. Eggeling, and S. W. Hell, "Two-Color Far-Field Fluorescence Nanoscopy," *Biophys. J.* **92**, L67-L69 (2007).
15. S. W. Hell, "Strategy for far-field optical imaging and writing without diffraction limit," *Phys. Lett. A.* **326**, 140-145 (2004).
16. B. Harke, J. Keller, C. K. Ullal, V. Westphal, A. Schonle, and S. W. Hell, "Resolution scaling in STED microscopy," *Opt. Express* **16**, 4154-4162 (2008).
17. M. Bates, T. R. Blosser, and X. Zhuang, "Short-Range Spectroscopic Ruler Based on a Single-Molecule Optical Switch," *Phys. Rev. Lett.* **94**, 108101(1-4) (2005).
18. M. Bates, B. Huang, G. T. Dempsey, and X. Zhuang, "Multicolor Super-Resolution Imaging with Photo-Switchable Fluorescent Probes," *Science* **317**, 1749-1753 (2007).
19. G. H. Patterson and J. Lippincott-Schwartz, "A Photoactivatable GFP for Selective Photolabeling of Proteins and Cells," *Science* **297**, 1873-1877 (2002).

1. Introduction

It is known that the resolution of every optical system, whether imaging or other, is restricted by the physical characteristics of its components. For far-field optical microscopy, this limit, relating the optical wavelength and the numerical aperture of the excitation with the achievable resolution $d = \lambda/2NA$ was originally formulated by Abbe. Since most of the microscopy in life sciences is done using imaging with conventional lenses and visible light, breaking this diffraction barrier of imaging is of high scientific priority. In the last decade, several realizations of far field fluorescence microscopy beyond the diffraction limit have been proposed (see review in [1]). It was shown that in multiphoton optical microscopy, Abbe's limit can be surpassed using optical nonlinearity. There, the improvement in resolution is typically proportional to the square root of the order of the nonlinear process used [2]. Due to the low order of the nonlinearity (typically second or third), and the use of long wavelength illumination, the resolution is not significantly improved. Existing schemes which significantly exceed Abbe's limit can be divided into two categories. The first involves methods with the capability of switching a single emitter between "on" and "off" states. These schemes such as STORM [3, 4] and PALM [5, 6], (and other methods using similar principles [7, 8, 9]) rely on statistical readout of a single emitter at a time, and record its position given a good enough signal to noise ratio.

The second category of methods uses ensemble "off" switching of emitters, where due to a strong depletion process of the surrounding fluorophores, emission is allowed only from a sub-diffraction limited spot. The most prominent of the latter category is STED [10], in which stimulated emission is used to deplete the excited state of a fluorophore. In the following, we first elaborate on some of the details of saturated depletion based microscopy, and then proceed to discuss the possibilities for its realization using a single-color single-beam excitation. In a STED microscope and its analogs, fluorophores are excited by a diffraction-limited excitation beam. This beam is combined with a doughnut shaped depletion beam having a single intensity zero at the center of the focal spot. Upon saturation of the depletion beam, fluorescent emission is limited to a sub-diffracted limited volume around this spot. In STED, the depletion mechanism relies on stimulated emission from the excited state. Thus, in a typical STED set up (see [1] and references therein), both the excitation beam and the depletion beam are ultrafast, in order for depletion to occur on a time scale much shorter than the radiative lifetime of the excited state, which is typically of the order of 1 nanosecond. While an all continuous-wave (CW) implementation of STED has been also realized [11], it was shown that this requires a significantly higher power than an equivalent pulsed realization. Recently, depletion mechanisms other than stimulated emission have been demonstrated involving optical pumping to a "lossy" channel. These include repumping of an emitting doped quantum dot from the emitting dopant state to the host [12], and utilizing optical shelving through a long lived triplet level of fluorophore for depletion [13]. The above reviewed STED schemes require a two beam set up which is based on either a careful synchronization [1, 12, 13] of the beams, or a high power STED beam [11].

This imposes significant limitations on extensions of STED such as for applications requiring two-color emission, which currently requires a delicate choice of fluorophores and a four color excitation scheme [14].

In this article we explore a theoretical scheme for a single beam single color saturated depletion based microscopy. It is based on a photo-switchable fluorophore which exhibits depletion of light emission upon saturation. In particular, we consider the case where the transition between the on and the off state is instantaneous and triggered solely by an increased excitation intensity.

This suggests a significant simplification over previous schemes, eliminating both requirements for synchronization between the depletion and excitation beams, and somewhat alleviating the requirements of having a zero of the intensity at the illumination center. A simple mathematical model is introduced and the width of the super resolved emission is calculated taking into account a two dimensional doughnut shaped intensity illumination.

2. Fluorophores exhibiting depletion of emission upon saturation

Consider a saturable fluorophore under pulsed excitation. This results in a distribution of emission probability $P_{em} = 1 - e^{-I/I_{em}}$, where I is the excitation intensity at a given wavelength and I_{em} the saturation intensity. Further more, assume this fluorophore has not only an emitting center, but also a depletion center (triggered by absorption at the same wavelength) with a saturation threshold $I_d > I_{em}$, so that only for fluorophores in which the depletion center is not excited, light emission is possible. The depletion mechanism can be therefore taken into account by multiplying the emission probability with the number of the un-depleted fluorophores. The final emission probability is given by

$$F(I) = (1 - e^{-I/I_{em}}) \cdot e^{-\frac{I}{I_d}}. \quad (1)$$

The simple model above assumes that depletion by excitation of the depletion center is efficient, i.e. depletion occurs on a time scale much shorter than both the radiative lifetime of the fluorophore and the relaxation time of the depletion center. We assume nothing further on the dynamics of the depletion mechanism, although clearly it has to be reversible within the time delay between two consecutive pulses for the presented calculation to be exact.

In Fig. 1(a) we plot Eq. (1) for several values of $\alpha = I_d/I_{em}$, with $I_{em} = 0.01$ fixed. Upon increasing the excitation energy we observe a linear increase of the emission as long as we are far enough from both the depletion threshold and saturation. As the excitation power approaches the depletion threshold, the emission starts to drop, creating a maximum at $I_0 = I_{em} \ln(1 + \alpha)$. The value of the emission at the maximum depends only on α and is given by:

$$F_m(\alpha) = \frac{\alpha}{1 + \alpha} \cdot \frac{1}{1 + \alpha}^{\left(\frac{1}{\alpha}\right)}. \quad (2)$$

This function, plotted in Fig. 1(b), is a monotonically increasing function of α and approaches the value of unity at infinity. For small α , the fluorophore will be efficiently depleted even for smaller values of the excitation energy, however the emission maximum will be relatively small as can be seen in Fig. 1(b). On the other hand, a large value of α would mean an increased effective quantum yield of the fluorescence but would require excessive energy to achieve saturation. In the following we tune α to a characteristic value for which $F(\alpha_h) = 0.5$, corresponding to $\alpha_h \simeq 4$.

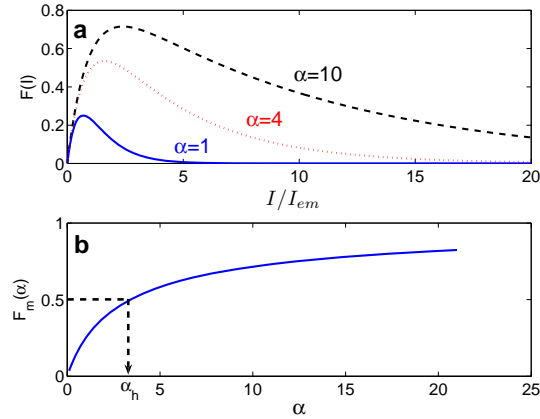


Fig. 1. Properties of a fluorophore exhibiting depletion upon saturation. a) Emission intensity (normalized to an undepleted fluorophore) as a function of excitation intensity for several values of α . b) The maximal emission yield (relative to an undepleted fluorophore) as a function of α .

3. Application for sub-diffraction limited imaging

In order to obtain a sub-diffraction emission profile from the fluorophore, consider a two dimensional sample which is illuminated with a (strong) doughnut shaped excitation, to which a (weak) gaussian centered at the doughnut zero is added (in practice this requires that the intensity zero is spoiled). Both components have a width Γ

$$I(r) = I_{max} \cdot \frac{e}{4} \cdot \left(\frac{8r^2}{\Gamma^2} e^{-2\frac{r^2}{\Gamma^2}} + \delta e^{-2\frac{r^2}{\Gamma^2}} \right), \quad (3)$$

where $r^2 = x^2 + y^2$.

As was shown in Fig. 1, in order to obtain maximum fluorescence at the center of the beam, we have to tune the constant δ to fulfill $I(0) = I_0$, this gives

$$\delta = \frac{4}{e} \frac{I_{em}}{I_{max}} \ln(1 + \alpha). \quad (4)$$

From this point onward we thus fix δ according to Eq. (4). A cross-section of this input beam is plotted (blue/dash-dot) in Fig. 2 along the X-axis. As can be seen at the inset of Fig. 2, it is non-vanishing at the center. Thus, emission will take place in a restricted area around the origin. However, in the surrounding region, where the intensity is above the depletion threshold, fluorescence will be quenched. Further outward from the center ($r > \approx 2\Gamma$) the input intensity again falls below the depletion threshold, resulting in the appearance of a 2D ring-shaped fluorescence. Since depletion around the central lobe is saturated, the mechanism by which its width is narrowed down is analogous to the STED mechanism [10]. Similarly, there is, in principle, no theoretical lower bound for the width of the central lobe.

The sample is excited by focusing the input beam so that at the focus the excitation profile is given by Eq. (3). The fluorescence (black dashed line in Fig. 2) is collected using the same lens which has a diffraction-limited excitation spot size Δ . Clearly, in order to be able to resolve the sub-diffraction limited central peak from the outer ring using the same lens, two conditions have to be met: First, the width of the beam at the focus has to be larger than the diffraction limited spot size of the lens, namely $\Gamma > \Delta$, this necessarily means that the excitation beam *must not* fill the whole back aperture of the lens. Second, detection through a confocal aperture

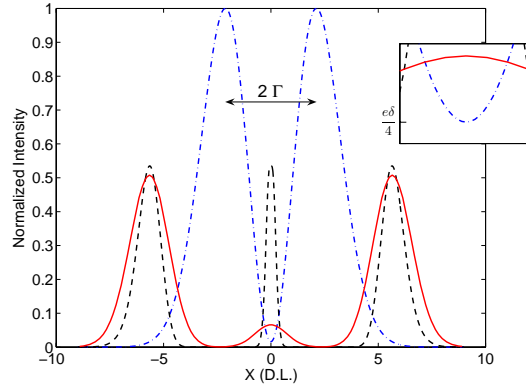


Fig. 2. Excitation and (dashed-dot blue line) and emission profiles (dashed black line) along the X axis for a fluorophore exhibiting emission depletion upon saturation. The overall detected intensity through a confocal pinhole as a function of its position along the X axis (solid red line), exhibiting deep dips between the central lobe and the sidelobes, shows clearly that at $x=0$ efficient rejection of the sidelobe emission is possible. The inset shows a blow up of the origin to emphasize that the illumination pattern (blue/dash-dot) is non-vanishing at the center. The parameters used for this plot are ($I_d/I_{max} = 0.04$, $\Gamma/\Delta = 3$ and $\alpha = 4$)

is required, such that the detection point spread function (PSF) would overlap only the central lobe. Assuming that the detection PSF is a Gaussian of the form e^{-r^2/Δ^2} , we plot in Fig. 2 the total collected signal as a function of the pinhole position along the x-axis (solid red line). The observed dips separating the central lobe from the sidelobes clearly show that under these conditions (where we have chosen $\Gamma = 3\Delta$) the central lobe emission can be effectively isolated. Although sidelobe rejection can be less efficient for other choices of the detection PSF, such as in the limit of a small pinhole (not shown), the contrast between the central lobe emission and the sidelobe background is still about an order of magnitude under the conditions of the current example.

Assuming that $I_d, I_{em} \ll I_{max}$, then up to first order, the width X_w of this central lobe is given by

$$M \equiv \frac{X_w}{\Delta} \cong \frac{\Gamma}{\Delta} \sqrt{\frac{I_d}{2e \cdot I_{max}}} \sqrt{1 + \ln\left(\frac{1 + \alpha}{\alpha}\right)}, \quad (5)$$

which is similar to the result obtained by Hell and coworkers in [15, 16].

In practice the spatial resolution depends only on two parameters: the saturation ratio I_{max}/I_d and the amount of underfilling the objective back aperture Δ/Γ . Note that this factor depends on the details of the excitation pattern. As expected, it shows an inverse square root dependence on the saturation ratio and a linear dependence on the underfilling factor. The dependence on α is very weak within a reasonable parameter range. For the parameters used in Fig. 2 ($I_d/I_{max} = 0.04$, $\Gamma/\Delta = 3$ and $\alpha = 4$), $M=0.3$, which corresponds to a three-fold increase in the resolution beyond that achievable with diffraction-limited illumination.

Figure 3(a) shows the width of the central lobe (blue/dash) in units of the diffraction limited spot as a function of the depletion threshold, divided by the peak intensity of the excitation beam. This was calculated numerically taking into account the profile of the emission. As expected from Eq. (5) the curve has a square root dependence on the saturation level. On the other hand, at lower maximum energy we will obtain an emission central lobe larger than Δ . In order

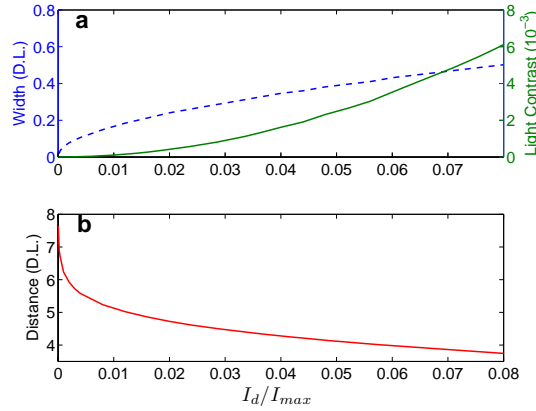


Fig. 3. a) The width of the central lobe and the light contrast (ratio of signal in the central lobe to that in the outer ring) as a function of the excitation intensity. b) the distance from the central lobe to the peak emission in the outer ring as a function of excitation intensity.

to assess the required efficiency of rejection of the outer ring luminescence, we also plot in Fig. 3(a) the light contrast (green/solid). This is defined to be the power contained in the central (confocal) lobe divided by the power within the sidelobe. As can be seen, up to nearly an order of magnitude improvement in spatial resolution is achievable in a reasonable parameter range ($10^{-3} - 10^{-2}$). The distance of the outer ring from the central lobe is also plotted as a function of the depletion intensity (Fig. 3(b)). It is important to note that although the distance between the central and side lobes decreases with the depletion intensity, the light contrast is improved, and the detection is made simpler.

4. Discussion

The suggested scheme is, in practice, a simplified variant of saturated depletion based microscopy [1]. Its main advantage over other realizations of depletion-based microscopy is in the simplicity. Both the excitation and depletion beams are combined into a single excitation beam, and the restriction on having a true zero in the depletion beam is relaxed. However, these simplifications come with the added complexity of efficiently rejecting the outer ring emission, and avoiding the enhanced photobleaching due to it. Both these problems can be overcome by the use of multipoint illumination (that is, an array of nearly dark points separated by more than the diffraction limit) [1]. Further more, such an illumination will increase both the spatial resolution and the signal-to-background ratio of our suggested scheme.

The scheme we suggest utilizes pulsed excitation. A direct application of this idea to CW excitation is impossible. This can be explained by solving the rate equations for our case. In their simplest form the rate equations are

$$\frac{dN_R}{dt} = -\frac{N_R}{\tau_{rad}} - \frac{N_R N_D}{\tau_{dep}} + \alpha I(1 - N_R) \quad (6)$$

$$\frac{dN_D}{dt} = -\frac{N_D}{\tau_{rel}} + \beta I(1 - N_D) \quad (7)$$

where N_R and N_D are the fractions of excited emitting centers and depleting centers, respectively, τ_{rad} the radiative lifetime of the fluorophore, τ_{dep} the response time of the depletion center, τ_{rel} the relaxation time of the depleting center and α and β the respective absorption cross sections. The two equations above are coupled by the second term on the right of Eq. 6,

which enables the depletion of N_R over a time scale given by τ_{dep} . The pulsed excitation analysis presented throughout this paper requires that $\tau_{rel}, \tau_{rad} \gg \tau_{dep}$ (and, of course, an excitation pulse shorter than τ_{dep}) and assumes a given ratio β/α . Under CW excitation, however, the steady-state solution of this system is:

$$N_R = \frac{\tau_{rad}\alpha I}{1 + \frac{\tau_{rel}\beta I \tau_{rad}}{(1+\tau_{rel}\beta I)\tau_{dep}} + \tau_{rad}\alpha I} \quad (8)$$

which does not exhibit emission depletion upon saturation. Intuitively, this can be understood considering the following: Under pulsed excitation, both the emission and depletion centers are excited at the same time. As a result, excitation of the emitting center is always followed by a rapid depletion. On the other hand, under CW pumping, excitation of the two centers is uncorrelated. This results in the emission expression given in Eq. (8), which is an increasing function of the intensity and is saturated at high enough intensities. In practice, the condition on τ_{dep} given in the introduction dictates the pulse lengths to be used in any experimental realization. In order to have an efficient depletion process ($\tau_{rad}/\tau_{dep} > \sim 1000$), the pulse length should be as short as a few picoseconds when using organic dyes, or tens of picoseconds for inorganic fluorophores such as quantum dots, which typically exhibit longer radiative lifetimes.

Although the experimental realization of the above scheme requires fluorophores with unusual optical characteristics, we believe such a fluorophore can be designed. For example, recent advances in design of reversibly photobleachable organic fluorophores, which are based on two coupled systems such as the system of two cyanine dyes [17, 18] or modified fluorescent proteins [19] show a promising route towards the synthesis of such systems. Other alternatives include designed inorganic fluorophores, particularly semiconductor quantum dots, where two-color reversible photobleaching has already been demonstrated [12]. To summarize, we have presented a theoretical framework for a simplified version of depletion-based microscopy, which, utilizing a designed intensity response of the fluorescence, exhibiting emission depletion upon saturation, alleviates some of the difficulties associated with current multicolor or time-multiplexed multibeam excitation geometries.

Acknowledgments

This research was supported by the Israel Science Foundation (grant No. 596/07) and by the Minerva foundation, with funding from the Federal German Ministry for Education and Research.